

Acceleration parameters for fluid physics with accelerating bodies

I.M.A. Gledhill¹, H. Roohani², A. Biobaku² and B. Skews²

¹Aeronautical Systems Competency Area, DPSS, CSIR. PO Box 395, Pretoria 0001

²School of Mechanical, Industrial and Aeronautical Engineering, University of the Witwatersrand, Johannesburg

E-mail: igledhil@csir.co.za

Abstract. Theoretical work on transforming the Navier-Stokes equations into arbitrarily accelerating frames has included the continuity, momentum, and energy conservation equations. An analysis of the momentum equation in non-dimensional terms leads to an acceleration parameter that appears to be new in fluid physics, but is known in cosmology. A selection of cases for rectilinear acceleration has been chosen to illustrate the point that this parameter alone does not govern regimes of flow about significantly accelerating bodies, and reference must be made, above all, to the Mach number for transonic effects. Other parameters from the literature on impulsive start-up in wind tunnels are also shown to be useful in delimiting regimes of flow, such as the Freymuth start-up time. Two dominant effects in fluid dynamics with accelerating objects are shown to be flow history, a term being used to cover the difference between an instantaneous flow field with an accelerating body and the flow field about the same body at steady state, and the dependence of stagnation pressure on acceleration. The dependence of these effects on dimensionless parameters is explored.

1. Introduction

Increased agility is a topic of growing importance in aeronautics. In the design of aircraft, missiles, and Unmanned Aerial Systems, growing emphasis is being placed on the ability to out-maneuvre another vehicle. Current missiles are launched under an acceleration of about 200 g , where g is the acceleration due to gravity, and may turn at 100 g . Earlier missiles have been ground-launched at 400 g . Accurate prediction of the transient loads using Computational Fluid Dynamics (CFD) is being explored, and in addition, methods of distinguishing regimes in which the aerodynamic effects of acceleration are significant are required in order to guide conceptual design.

Earlier reports and papers have provided theoretical support in the form of transformation of the Navier-Stokes equations between inertial and non-inertial frames [1,2,3,4] for arbitrary acceleration. A source term appears in the momentum equation in the non-inertial frame for linear acceleration. The magnitude of the linear acceleration term may be compared to that of the convection term, and provides a coefficient Q ; a description is provided below. We term Q the acceleration parameter. In

addition, some guidance on low acceleration effects is available from experimental work on transient effects in the start-up of wind tunnels, and this work provides the Freymuth start-up time $t_F = \sqrt{L/a}$ [5]. These parameters are confined to a linear comparison of acceleration effects with convective phenomena.

In compressible flow with speed $v(t)$ and sound speed c , the Mach number, $M(t) = v(t)/c$, is of dominant importance. For the present applications, constant acceleration along the axis of the flare body, shown in figure 1, from $M = 0.1$ to $M = 1.0$ is modelled. A uniform acceleration of $\dot{M} = 3 \text{ s}^{-1}$ or $a_0 = \dot{v}(t) \sim 1041 \text{ ms}^{-2}$, is modelled. Work in this paper is intended to contribute to understanding regimes of accelerating aerodynamics using Q , t_F and the Mach number.

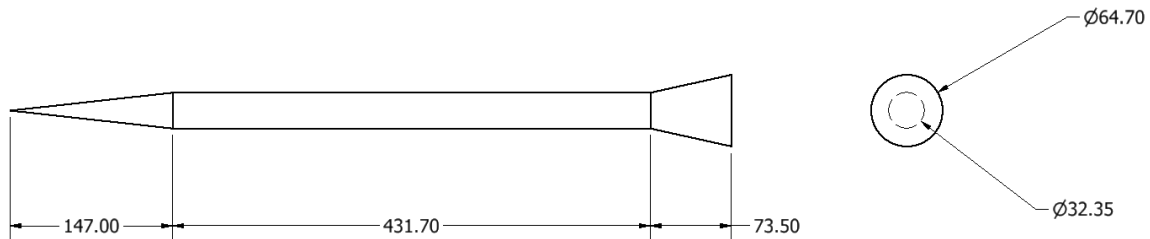


Figure 1. Flare geometry. Dimensions are in mm.

Dimensionless parameters only compare terms in the governing equations and do not describe the complicated non-linear behaviour of compressible fluids. The term flow history was introduced by Bassett [6] in connection with boundary layer development. Lilley showed flow history in compressible fluids using the Mach lines of a single particle [7]. After this paper, very little work was done analytically, and experiments have been very difficult to set up. For shapes of real interest it is necessary to explore the relevant flow fields with CFD. Roohani and Skews [8,9,10] have modelled objects of various shapes with CFD and provided evidence of flow history and inertial effects. Flow history can be visualised in terms of a lag between the current flow field and earlier flow fields. In other words, the current flow field reflects some of the unresolved features of earlier flow fields.

In this paper, the results of CFD calculation of drag forces on a slender body of rotation are discussed in order to explore regimes in which acceleration effects are easily categorised with flow parameters. The flare configuration has been explored by Forsberg *et al.* [3] and it was shown that for the specific case investigated, unsteady drag dropped in comparison with steady results through the transonic region. In work on aerofoils, shocks appear on curved surfaces in the transonic regime or as detached bow shocks at $M > 1$. The flare, by contrast, has a conical nose, on which attached oblique shocks should develop, and has expansion and compression corners at the nose and tail flare.

2. Theory

In an inertial frame Σ , the Navier-Stokes equations are the conservation laws for mass, momentum and energy. Transformation of mass and momentum conservation equations to an arbitrarily moving non-inertial frame Σ' is given by Forsberg [2]. For linear acceleration a_0 of the origin O' of Σ' relative to the origin O of Σ , an acceleration source term appears in frame Σ' . The equation is normalized to typical parameters, so that the coefficient of the convective term is 1. The coefficient of the time derivative term becomes the Strouhal number, $St = \frac{v_0 t_0}{L}$. The coefficient of the acceleration term is the acceleration parameter $Q = \frac{L a_0}{v_0^2}$ where L is a typical length and v_0 is a typical velocity; this parameter provides a linear estimate of the importance of acceleration-related effects in comparison to convective

flow. Inclusion of gravity \mathbf{g} as an external force in Σ leads to an analogous term characterized by the Froude number, $Fr = \frac{v_0}{\sqrt{Lg}}$. The parameter Q is related to Fr^{-2} .

Typical length L is defined as the length of the flare and is shown with other parameters in Table 1. The pressure and temperature used were 101325 Pa and 300 K respectively. The Freymuth start-up time is an estimate of the time taken to traverse length L at acceleration a_0 , starting from rest. It has been used as a normalising factor in examining the transient vorticity developing over aerofoils in wind-tunnel start-up studies, with a_0 referring to the flow acceleration. While this case is not equivalent to the acceleration of an object from rest, an object accelerating from rest in still air would take of the order of the Freymuth time to travel its own length L , and the factor may therefore be taken to be an indicator of the minimum time during which start-up transients may be expected. The Freymuth time indicates that start-up transients over this flare may be expected to last for 0.03 s, or when $M \sim 0.23$ in the present flare case.

Table 1. Typical parameters

Parameter	Value
Typical length L	652.3 mm
Sound speed c	347 ms ⁻¹
Initial Mach number M_0	0.10
Typical Mach number M	1
Typical acceleration a_0	1041 ms ⁻²
Acceleration parameter $Q = \frac{La_0}{v_0^2}$	0.26
Freymuth start-up time $\sqrt{L/a_0}$	0.03 s

It is noted that at the slender conical nose with an attached oblique shock, stagnation properties are an approximation to surface pressures that are likely to be modelled.

3. Methodology

The model geometry is shown in figure 1. The primary interest of this model is in examining shocks, surface pressures and drag, and it is reasonable to use an axisymmetric approximation which will eliminate asymmetric vortex shedding in the wake.

The acceleration terms for the momentum and energy were provided as source terms in the non-inertial frame Σ' through user coding in a finite-volume cell-centred unstructured code ANSYS[®] Fluent. A second-order upwind scheme was used for shock capture. A two-dimensional hybrid quadrilateral-triangular unstructured grid, with adaptive mesh refinement, was used, and local Reynolds numbers y^+ were checked at the wall for compatibility with the Spalart-Allmaras turbulence scheme, which was chosen as a well-validated model in the transonic regime. The far field boundaries receive relative velocities that increase with the acceleration a , while the walls are no-slip walls with velocity zero relative to the body. Mesh independence was established to a level of 5% variation in loads between successive grids. A time step of 10^{-4} s was found to be small enough to capture the same loads and flow fields as time steps less than 10^{-4} s. A grid convergence study was performed on the global mesh size before checking results for pressure along the missile wall with adaptive gridding on the steady state solutions. Grid adaption was performed every 10 time steps in the transient solutions. Verification of the source terms was performed by inspecting the evolution of the pressure field across the domain.

4. Results

Drag is not normalized in acceleration cases, but presented in Newtons.

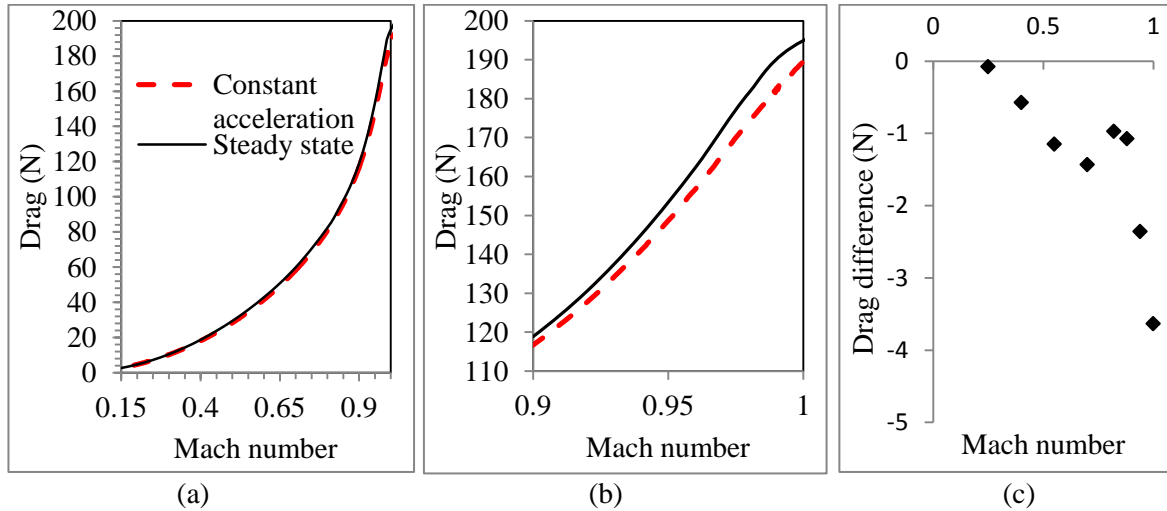


Figure 2. Drag and drag difference as a function of Mach number

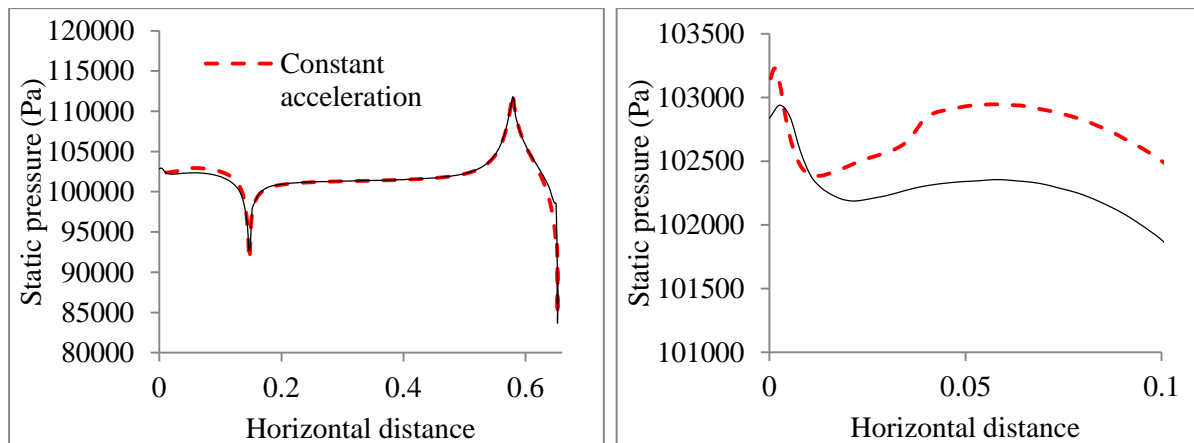


Figure 3. Pressure profiles for $M=0.7$ as a function of distance from the nose over (a) the length of the flare and (b) the stagnation region

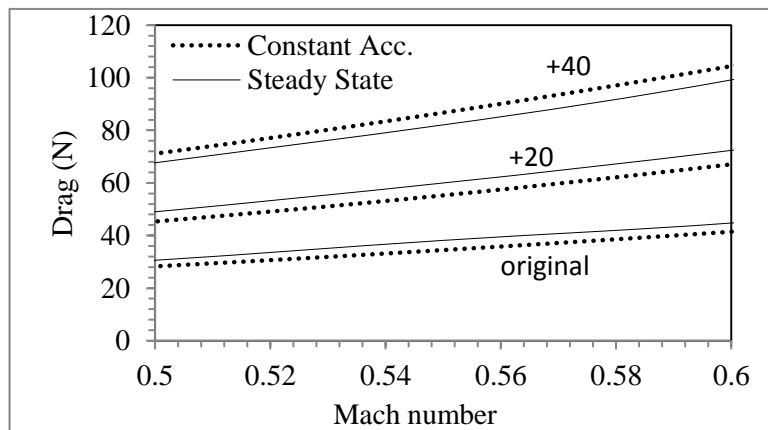


Figure 4. Drag in the subsonic region for increased calibre geometries

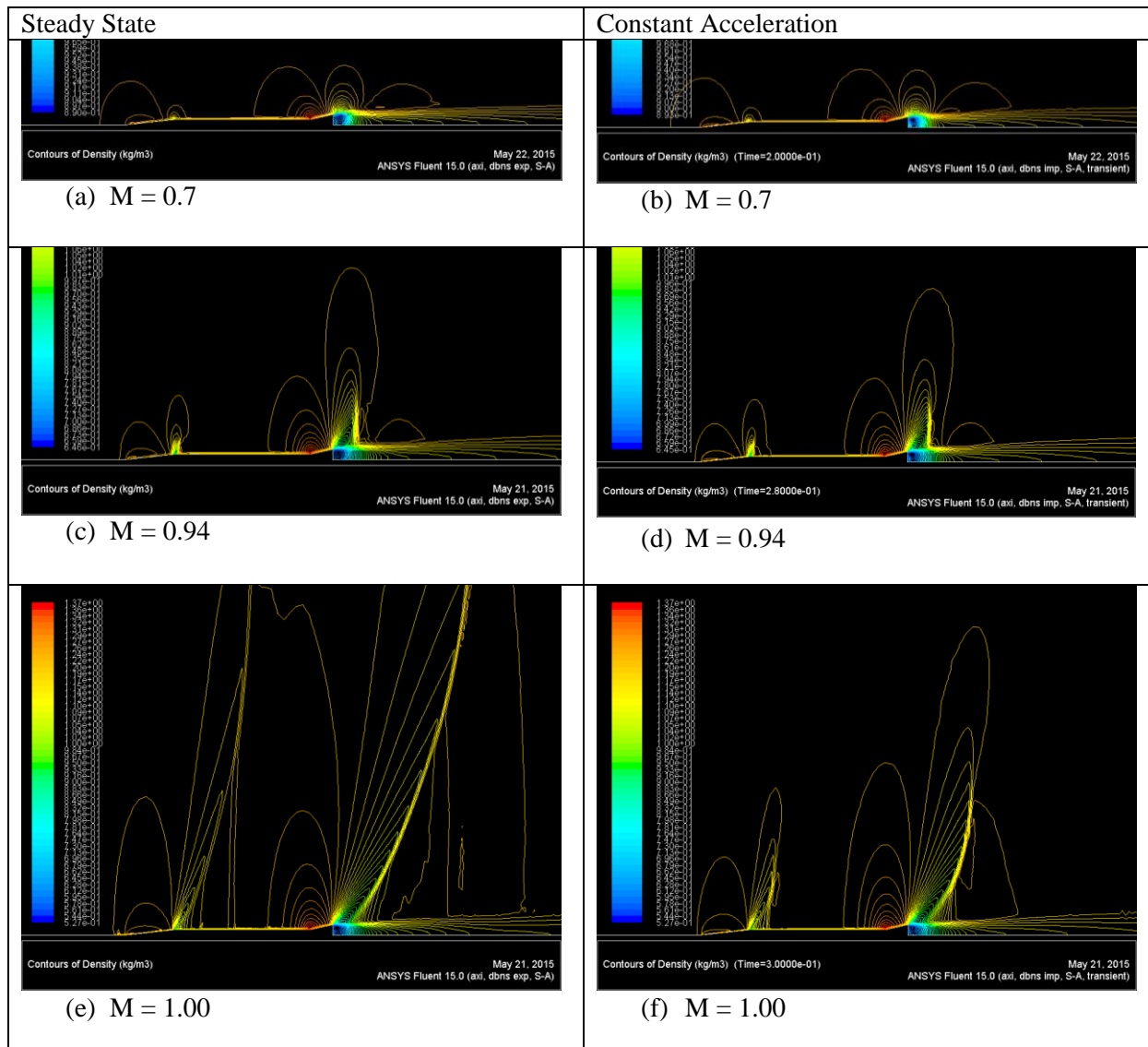


Figure 5. Instantaneous density flow fields. Left: steady state. Right: constant acceleration

5. Discussion of results

Figure 2 compares steady and unsteady drag at Mach numbers in the subsonic and transonic range. It is clear that for this particular geometry drag is usually lower in the unsteady case during acceleration. However, in previous work by Roohani and Skews [8,9,10] the opposite effect was observed in aerofoils and bluff bodies. This is because unsteady drag is not only a function of Mach number and acceleration, but it is also affected by the geometry of an object. In Figure 4 this phenomenon is illustrated by increasing the diameter of the flare by 20 mm and 40 mm and subjecting it to the same steady and unsteady conditions. It is shown that when the diameter is increased by 40 mm, acceleration results in an increase in drag compared to the steady state scenario. In figure 3 the pressure profile at Mach 0.7 as a function of distance from the nose shows that in the frontal area of the flare the pressure has increased due to acceleration. This is due to fluid inertia. At the tail flare the pressure is lower during acceleration, which can be attributed to flow history and boundary layer effects. At the flat base surface the minimum pressure during acceleration (84.5 kPa) is higher than the

minimum steady state pressure (83.4 kPa). Both these effects contribute to the lower drag observed during acceleration. Contours of density are shown in figure 5, where the steady state and the accelerating cases are compared at specific Mach numbers. At Mach 0.94 a recovery shock has developed in the wake of the flare in both cases. There appears to be a shock developing behind the expansion corner on the nose cone, which could be attributed to a separation bubble. This needs more detailed investigation as it appears to be a function of acceleration. In addition, the wake shock has strengthened in both cases, but extends a smaller distance from the centerline in the accelerating case. The decreased wave drag accounts for the sharp drop in drag for the accelerating case in the transonic region, shown in the data of figure 2(c).

The Freymuth time, which is a measure of the time in which start-up transients would be expected, is 0.03 s in this case, and the total trajectory is covered in 0.3 s. The start-up transients were not observed to be significant under these circumstances.

6. Conclusions

It has been shown that for a slender body of rotation, drag under acceleration of 1041m/s^2 from $M = 0.1$ is lower than drag in steady flow across the subsonic region, and that there is a significant decrease in unsteady drag near Mach 1. This is in contrast with previous work on aerofoils and bluff bodies. It is also shown that increasing the diameter of the slender body reverses the trend, so that drag under acceleration in the subsonic region is larger than steady drag. The decrease in drag is attributed to the effects of flow history over the rear of the flare body, including a decrease in wave drag as the wake shock is reduced in extent during acceleration. In these cases, flow history dominates flow inertia. However, as the diameter of the flare body is increased, flow inertia effects on the nose cone increase and dominate flow history effects, and the total drag rises above that of the steady state.

In this case, the Mach number is a clear indicator of changing compressible effects near Mach 1, where drag changes are very significant. The acceleration parameter Q is 0.26 based on the initial velocity, and very significant acceleration effects have been observed. This factor should be explored further in future work as an indicator of the relative significance of acceleration in understanding flow fields and aerodynamic loads.

References

- [1] Löfgren P 1998 *Relative Motion in Fluid Mechanics* FFAP-B-066 (Stockholm: Flygtekniska försöksanstalten, The Aeronautical Research Institute of Sweden)
- [2] Forsberg K 1999 *Treatment of a moving reference frame for discretized NS equations* (Stockholm: Flygtekniska försöksanstalten, The Aeronautical Research Institute of Sweden)
- [3] Forsberg K, Gledhill I M A, Eliasson P and Nordström J 2003 Investigations of acceleration effects on missile aerodynamics using CFD 2003 (American Institute of Aeronautics and Astronautics) *AIAA-2003-4084*
- [4] Gledhill I M A, Forsberg K, Eliasson P, Baloyi J and Nordström J 2009 Investigation of acceleration effects on missile aerodynamics using computational fluid dynamics *Aerospace Science and Technology* **13** 197–203
- [5] Freymuth P, Bank W and Palmer M 1983 Visualization of accelerating flow around an airfoil at high angles of attack *Z. Flugwiss. Weltraumforsch.* **7** 392–400
- [6] Basset BA1888 *Treatise on Hydrodynamics* (Cambridge: Deighton, Bell and Co.)
- [7] Lilley GM, Westley R, Yates AH and Busing JR 1953 Some aspects of noise from supersonic aircraft *J. Royal Aeronautical Soc. College of Aeronautics Report* **71** 396-414
- [8] Roohani H and Skews BW 2008 Unsteady aerodynamic effects experienced by aerofoils during acceleration and retardation *Proc. I. Mech.E.* **222** 631–636
- [9] Roohani H and Skews BW 2009 The influence of acceleration and deceleration on shock wave movement on and around airfoils in transonic flight *Shock Waves* **19** 297–305
- [10] Roohani H *Aerodynamic effects of accelerating objects in air* 2010 PhD Thesis (Johannesburg: University of the Witwatersrand)